Electronic and optical properties of the 1*T* phases of TiS_2, $TiSe_2$, and $TiTe_2$

Ali Hussain Reshak and S. Auluck
Physics Department, Indian Institute of Technology, Roorkee (Uttaranchal) 247667, India
(Received 21 February 2003; revised manuscript received 18 June 2003; published 18 December 2003)

The electronic properties of the 1*T* phase of TiX_2 (X=S, Se, and Te) compounds are calculated using the full potential linear augmented plane wave method as embodied in the WIEN97 code. Our calculations show that all the compounds are semimetallic. The density of states at the Fermi energy $N(E_F)$, controlled by the overlap between the Ti *d* and *X p* states, increases from 0.35 to 0.9 to 1.6 states/eV unit cell as we go from S to Se to Te. We report calculations of the anisotropic frequency-dependent optical properties of these compounds and find excellent agreement with the available experimental data. The optical properties show three main structures that can be attributed to transitions between the *X p* states and the Ti *d* states.

DOI: 10.1103/PhysRevB.68.245113 PACS number(s): 71.15.−m

I. INTRODUCTION

The titanium dichalcogenide compounds TiX_2 (X=S,Se,Te) have been studied extensively because of their interesting structural and electronic properties. TiX_2 show a great potential for a variety of technological applications (Wilson and Yoffe[1]). These compounds consist primarily of a hexagonal sheet of Ti atoms sandwiched between two similar sheets of chalcogen (X) atoms, forming the basic X-Ti-X sandwich. The sheets are coupled by relatively weak van der Waals forces while the atoms within the sheet are coupled by strong covalent bonds. These compounds have highly anisotropic physical properties so much so that they can be regarded as two-dimensional solids. As a result of this the TiX_2 can be intercalated with foreign atoms and molecules leading to significant changes in their electronic properties and making them technologically useful. For example, the intercalation of lithium in TiS_2 has found use in lithium batteries.[2]

There exist a number of band structure calculations of the 1*T*-TiX_2 compounds. Umrigar *et al.*,[3] using the self-consistent linear augmented plane-wave (LAPW) scheme, showed that TiS_2 is semimetallic. This was in contrast to the optical measurements of Greenway and Nitsche,[4] which suggested that TiS_2 is a semiconductor with a gap of 1–2 eV. The optical data of Liang and others[5,6] could not resolve this discrepancy as it did not extend to low enough energies. Murray and Yoffe[7] have calculated the band structure of the titanium dichalcogenides using semiempirical tight binding parameters fitted to optical reflectivity and absorption data. From the measurements of the Hall coefficient, thermoelectric power and resistivity as a function of pressure, Klipstein and Friend[8] concluded that the band overlap between S 3*p* states and Ti 3*d* states increased at a rate 4.5 meV/kbar. This work also suggested that TiS_2 is a semiconductor with a gap of around 0.18 eV. Benesh, Woolley, and Umrigar[9] calculated the band structure of TiS_2 and $TiSe_2$ using the LAPW method as a function of pressure and confirmed this increase in band overlap. However, their calculations also gave a semimetallic state with a 0.24 eV (0.55 eV) overlap for TiS_2 ($TiSe_2$). The calculation of Fang, de Groot, and Haas[10] based on the augmented spherical wave (ASW) method and of Wu *et al.*[11,12] based on the linear muffin-tin orbital (LMTO) method show that TiS_2 is semimetallic. A pseudopotential (PP) calculation shows TiS_2 to be a semiconductor with an indirect gap of about 2 eV.[13] Leventi-Peetz, Krasovskii, and Schattke[14] have calculated the dielectric function (DF) for $TiSe_2$, using the extended linearized augmented plane-wave (ELAPW) and the empirical tight-binding methods. Kim *et al.*[15] have studied the electronic structure and chemical bonding in TiX_2 (X=S, Se, and Te) by a first-principles molecular orbital calculation using the discrete-variational cluster method and have also studied the intra- and interlayer chemical bonding properties using the bond overlap population. The valence-band structures are in good agreement with the experimental results obtained by x-ray photoemission spectroscopy. Recently Sharma *et al.*,[16] using the full potential linear augmented plane-wave (FPLAPW) method, showed that 1*T*-TiS_2 is semimetallic at ambient pressure in agreement with the earlier calculations based on the ASW (Ref. 10) and LMTO (Refs. 11 and 12) methods but in disagreement with the PP calculation.[13]

Measurement of the polarized x-ray absorption near-edge spectra,[17–19] thermoreflectance,[20] and infrared spectra[21] of these compounds in charged density wave (CDW) states have further contributed to interest in these compounds. Claessen *et al.*[22] and de Boer *et al.*[23] have studied the electronic structure of 1*T*-$TiTe_2$ by high resolution angle-resolved photoelectron spectroscopy (ARPES) and found agreement with the density functional band calculations. The results confirm the semimetallic nature of this material as due to an overlap of Te 5*p* and Ti 3*d* bands. Rossnagel *et al.*[24] applied the ARPES to map the shape of Fermi surface for $TiTe_2$. Perfetti *et al.*[25] have presented a combined angle-resolved photoemission spectroscopy and resistivity study of $TiTe_2$. From the analysis of the quasiparticle spectral line shape they evaluated the electron-electron, electron-photon, and impurity scattering contribution to the quasiparticle lifetime. Kidd *et al.*[26] have employed the angle-resolved photoemission to measure the band structure of $TiSe_2$ in order to clarify the nature of $(2\times2\times2)$ CDW transition. They find a very small indirect gap in the normal phase transforming into a larger indirect gap at a different location in the Brillouin zone.

The optical properties of the TiX_2 compounds have been

measured by several workers. Greenway and Nitsche[4] have measured the reflectivity of single crystals of TiS_2, $TiSe_2$, and $TiTe_2$ with the electric field vector $\vec{E}$ approximately perpendicular to the hexagonal **c** axis in the energy range 1–12 eV. Beal, Knights, and Liang[5] have measured the transmission spectra of TiS_2 and $TiSe_2$ at liquid-helium temperature with $\vec{E}\perp\mathbf{c}$ in the energy range 0.5–4 eV. Hughes and Liang[27] have measured the normal-incidence reflectivity spectra in the photon energy range 4.5–14 eV on single crystals of the TiS_2 and $TiSe_2$ with $\vec{E}\perp\mathbf{c}$. Bayliss and Liang[28] have measured the normal incidence reflectivity in the energy range 0.5 to 5 eV for TiS_2 and $TiSe_2$ with $\vec{E}\perp\mathbf{c}$ and $\vec{E}\parallel\mathbf{c}$. Bayliss and Liang[29] have obtained the optical joint density of states (OJDOS) functions from Kramers-Kronig analysis of reflectivity measurement for TiS_2 and $TiSe_2$ in the energy range 0.6–14 eV. Borghesi *et al.*[20,30] have measured the reflectivity spectrum in the 1–9 eV region for TiS_2 and $TiSe_2$ with $\vec{E}\perp\mathbf{c}$. Baldassarre, Cingdani, and Levy[31] have measured the saturation photoacoustic spectra in TiS_2, $TiSe_2$, and $TiTe_2$ at energies above the fundamental absorption edge. The dips in the photoacoustic spectra may be ascribed to optical reflection effects inherent to the band structure. They show that saturation photoacoustic spectroscopy is a useful alternative tool to reflectivity measurements.

It is clear from the above that there exist a large number of band structure calculations for the TiX_2 compounds. These calculations are in agreement with the various ARPES experiments. There also exist numerous measurements of the optical properties and a recent photoacostic measurement.[31] However, comparison with the calculated band structure is not as profuse as for ARPES. We hope that our work will fill this gap. We note that all the calculations of the electronic and optical properties are based on the muffin-tin approximation. It would, therefore, seem a natural extension to do more accurate calculations based on full potential methods. Most optical measurements are for $\vec{E}\perp\mathbf{c}$. Since the optical properties are anisotropic we hope that our work will lead to optical measurements for $\vec{E}\parallel\mathbf{c}$ so as to bring out this anisotropy a meaningful comparison with theory. It would also be interesting to study the effect of replacing S by Se and Te on the optical properties. With this in mind, we report calculations of the electronic and optical properties of TiX_2 compounds using the FPLAPW method[32] and compare with available data.

In Sec. II we give details of our calculations. The band structure and density of states are presented and discussed in Sec. III. The frequency-dependent dielectric function and other optical properties are given in Sec. IV, and Sec. V summarizes our conclusions.

II. DETAILS OF CALCULATIONS

In our calculations we use the FPLAPW method in a scalar relativistic version as embodied in the WIEN97 code,[32] including local orbitals for the high-lying ''semicore states.'' This is an implementation of the density-functional theory (DFT) with different possible approximations for the exchange-correlation (XC) potentials. The XC potential was constructed following Von Barth and Hedin.[33] Exchange and correlation are treated within the local-density approximation (LDA) and scalar relativistic equations are used to obtain self-consistency. The Kohn-Sham equations are solved using a basis of linear APW's. The potential and charge density in the muffin-tin (MT) spheres are expanded in spherical harmonics with $l_{\max}=8$ and nonspherical components up to $l_{\max}=6$. In the interstitial region the potential and the charge density are represented by Fourier series. We expected spin-orbit coupling to be important in $TiTe_2$, but have decided not to include this because in our previous work[34] on WSe_2 we find that the spin-orbit interaction has a minor influence on the optical properties.

TABLE I. Lattice parameters of TiX_2.

	TiS_2[a]	$TiSe_2$[b]	$TiTe_2$[c]
a (Å)	3.408	3.536	3.777
c (Å)	5.699	6.004	6.498
z	0.25	0.25	0.2628

[a]References 15 and 41.
[b]References 14 and 15.
[c]References 15 and 23.

TiX_2 (X=S,Se,Te) crystallizes in the $1T$ phase (space group $P\text{-}3m1$, no. 164). The Ti atom is at $1c$ (origin) and the two X atoms at $2d$ $\pm(\frac{1}{3}\frac{2}{3}\mathbf{z})$ positions. We have performed calculations at ambient pressure using the experimental lattice constants **a** and **c** for all compounds. The distortion from the octahedral configuration is expressed by the quantity **z**, the distance between Ti and the chalcogen plane in units of the lattice constant **c** perpendicular to the layers. For the value of **c** in the case of TiS_2/Se_2 and in-layer lattice constant **a**, it should be equal to 0.2404 in the ideal octahedral case, but actually is equal to 0.25.[14] For $TiTe_2$ we use the experimental value of **z**. In Table I we collect all the lattice parameters used in our work. Self-consistency was obtained using 100 and 200 k points in the irreducible Brilliuon zone (IBZ). Our calculations show that convergence is obtained with 100 k points (with respect to band structure and density of states). The BZ integrations were carried out using the tetrahedron method.[35] The frequency-dependent anisotropic optical properties are calculated using 200 and 500 k points in the IBZ. We find very small differences in the two calculations. We present calculations with 500 k points in this paper.

III. RESULTS AND DISCUSSIONS

A. Band structure and density of states

The band structure for $1T\text{-}TiS_2$, shown in Fig. 1(a) (our previous work[16]) is in agreement with the ASW calculation of Fang, de Groot, and Haas[10] and the LAPW calculation of Umrigar *et al.*[3] but is in disagreement with the pesudopotential calculation of Allan *et al.*[13] which predicts TiS_2 to be a semiconductor with an indirect gap of around 2 eV. The total density of states (DOS) along with the Ti $3d$, S $3s$, and S $3p$ partial DOS are shown in Fig. 1(a). From the partial DOS we

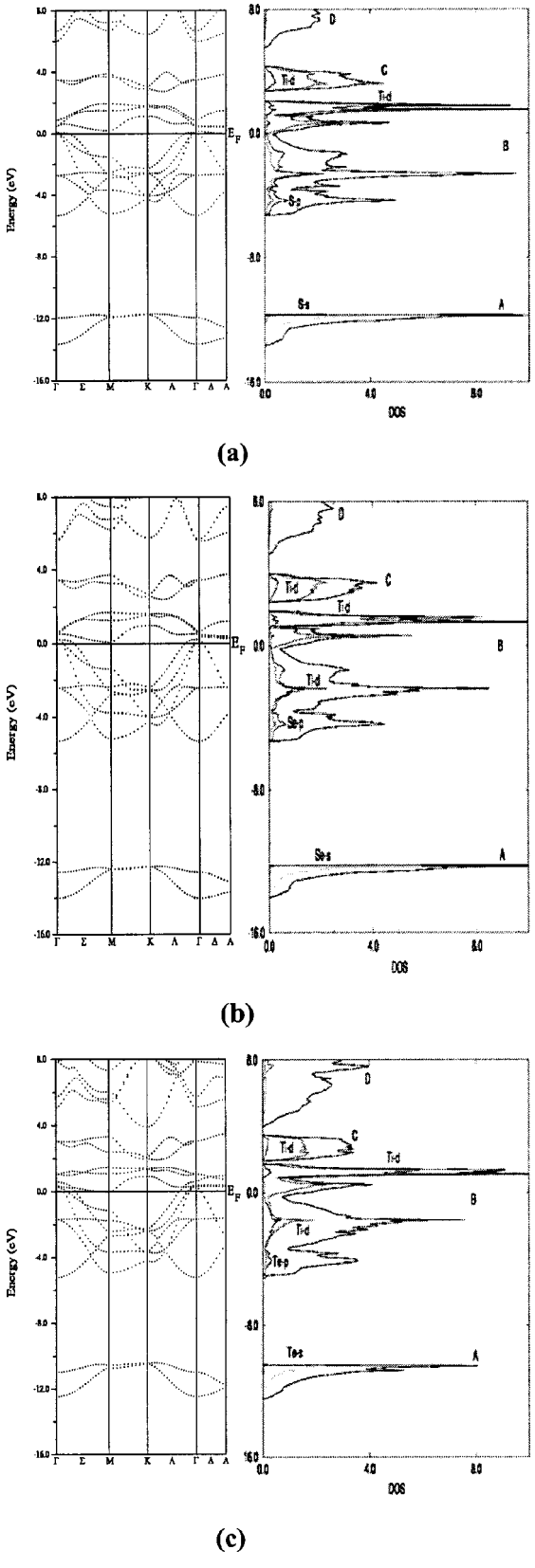

FIG. 1. Band structure and total DOS along with the partial density of states (states/eV unit cell), (-----) denotes S/Se/Te s states, (—·—·—·—) denotes Ti d states and (·····) denotes S/Se/Te p states. (a) $1T$-TiS_2. (b) $1T$-$TiSe_2$. (c) $1T$-$TiTe_2$.

are able to identify the angular momentum character of the various structures. The DOS at Fermi energy E_F is controlled by the overlap between the S $3p$ states (valence) and Ti $3d$ states (conduction). This overlap is small indicating a semimetallic state with a DOS at E_F, $N(E_F)$ of 0.35 states/eV unit cell in agreement with the value of 0.39 states/eV unit cell obtained by Takahira, Suzuki, and Motizuki[36] using the self-consistant APW method, and 0.37 states/eV unit cell obtained by Kim *et al.*[15] using the discrete-variational (DV)$-X\alpha$ cluster method. A strong hybridization is found between S p states and Ti d states below E_F.

The band structure of $1T$-$TiSe_2$ is plotted in Fig. 1(b). It is similar to the band structure of a previous ASW calculation by Fang, de Groot, and Haas[10] and ELAPW by Leventi-Peetz, Krasovskii, and Schattke[14] The calculation of Leventi-Peetz, Krasovskii, and Schattke shows more overlap between Se p and Ti d states around E_F. The lowest two bands (Se $4s$ states) are shifted towards lower energy by around 0.7 eV with respect to E_F in comparison with $1T$-TiS_2. The Se $4p$ bands are shifted towards higher energy by around 0.3 eV. The Ti $3d$ bands are shifted towards lower energy by around 1 eV. The DOS at Fermi energy, $N(E_F)$, is around 0.9 states/eV unit cell, in agreement with the calculations of Kim *et al.*[15] and smaller than the value of 1.5 states/eV unit cell obtained by Leventi-Peetz, Krasovskii, and Schattke.[14]

The band structure of $1T$-$TiTe_2$ is plotted in Fig. 1(c). The lowest two bands (Te $5s$ states) are shifted towards higher energy by around 1 eV with respect to E_F compared to $1T$-TiS_2. The Te $5p$ bands are shifted towards higher energy by around 0.5 eV with respect to E_F. The Ti $3d$ bands are shifted towards the lower energy by around 0.5 eV in agreement with the results of de Boer *et al.*,[23] Rossnagel *et al.*,[24] and Claessen *et al.*[22] The DOS at Fermi energy, $N(E_F)$, is around 1.6 states/eV unit cell higher than the value of 1.35 states/eV unit cell obtained by Kim, Mizuno, and Tanaka[15] and the value of 1.1 states/eV unit cell obtained by de Boer *et al.*[23] and lower than the value of 1.8 states/eV unit cell obtained by Claessen *et al.*[22]

IV. OPTICAL PROPERTIES

Measurement of the dielectric properties is normally done on single crystals. For compounds having hexagonal or tetragonal symmetry, the experiments are performed with electric field vector $\vec{E}$ parallel or perpendicular to the **c** axis.[37] The corresponding dielectric functions are $\epsilon^{\parallel}(\omega)$ and $\epsilon^{\perp}(\omega)$.

TABLE II. Peak positions of $\epsilon_2^{\perp}(\omega)$ and $\epsilon_2^{\parallel}(\omega)$ and plasma frequency for $1T$-TiX_2 compounds (all in eV).

	TiS_2	$TiSe_2$	$TiTe_2$
A	2	1.5	1
B	4.5	4	3.5
C	9.5	8.5	7.5
$\omega_P^{\parallel}$	0.87	1.94	2.63
$\omega_P^{\perp}$	1.18	2.60	3.37

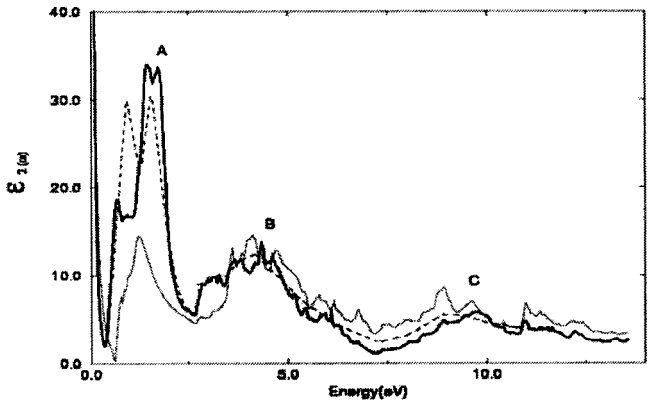

(a)

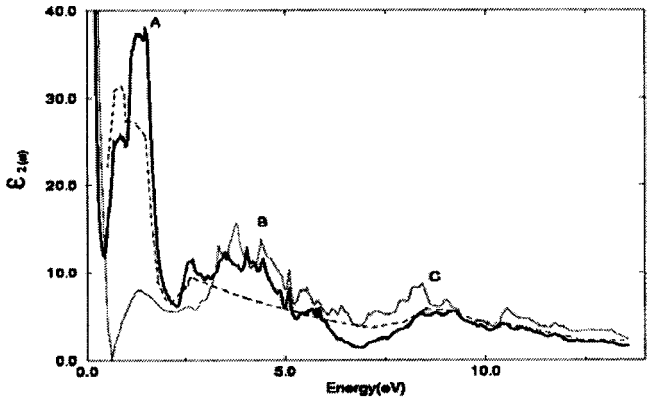

(b)

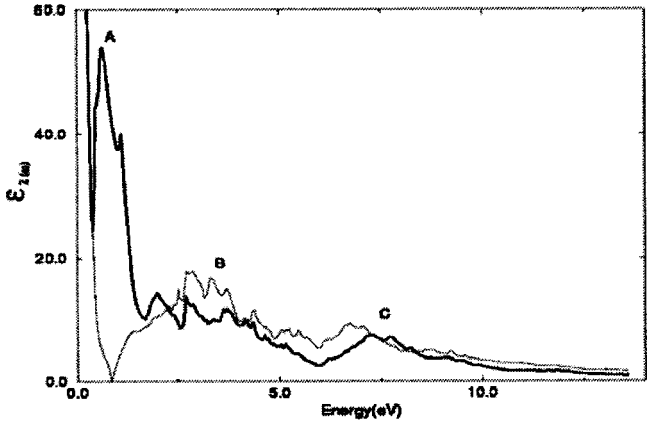

(c)

FIG. 2. Calculated $\epsilon_2^{\parallel}(\omega)$ (light line) and $\epsilon_2^{\perp}(\omega)$ (dark line) along with the experimental data (Ref. 29) (dashed line) for $\vec{E}\perp\mathbf{c}$. (a) $1T$-TiS_2, (b) $1T$-$TiSe_2$, and (c) $1T$-$TiTe_2$.

The calculations of these dielectric functions involve the energy eigenvalues and electron wave functions. These are natural outputs of band structure calculations. We have performed calculations of the imaginary part of the interband frequency dependent dielectric function using the expressions:[37]

$$\epsilon_{2\ \mathrm{inter}}^{\parallel}(\omega)=\frac{12}{m\omega^2}\int_{\mathrm{BZ}}\sum\frac{|P_{nn'}^{Z}(k)|^2 dS_k}{\nabla\omega_{nn'}(k)},$$

$$\epsilon_{2\ \mathrm{inter}}^{\perp}(\omega)=\frac{6}{m\omega^2}\int_{\mathrm{BZ}}\sum\frac{[|P_{nn'}^{X}(k)|^2+|P_{nn'}^{Y}(k)|^2]dS_k}{\nabla\omega_{nn'}(k)},$$

where the summation is over n and n'. The above expressions are written in atomic units with $e^2=1/m=2$ and $\hbar=1$. ω is the photon energy and $P_{nn}^{X}(k)$ is the $\mathbf{x}$ component of the dipolar matrix elements between initial $|nk\rangle$ and final $|n'k\rangle$ states with their eigenvalues E_nk and $E_{n'}(k)$, respectively. $\omega_{nn'}(k)$ is the energy difference

$$\omega_{nn'}(k)=E_n(k)-E_{n'}(k)$$

and S_k is a constant energy surface defined as

$$S_k=\{k;\omega_{nn'}(k)=\omega\}.$$

As the $1T$-TiX_2 compounds are semimetallic we must include the Drude term (intraband transitions[38])

$$\epsilon_2^{\perp}(\omega)=\epsilon_{2\ \mathrm{inter}}^{\perp}(\omega)+\epsilon_{2\ \mathrm{intra}}^{\perp}(\omega),$$

where

$$\epsilon_{2\ \mathrm{intra}}^{\perp}(\omega)=\frac{\omega_P^{\perp 2}\tau}{\omega(1+\omega^2\tau^2)},$$

where ω_P is the anisotropic plasma frequency[39] and τ is the mean free time between collisions.

$$\omega_P^{\perp 2}=\frac{8\pi}{3}\sum_{kn}\vartheta_{kn}^{\perp 2}\delta(\varepsilon_{kn}),$$

where ε_{nk} is $E_n(k)-E_{\mathrm{F}}$ and $\vartheta_{nk}^{\perp}$ is the electron velocity (in basal plane) squared. Similarly expressions for the parallel component can be written. The values of $\omega_P^{\parallel}$ and $\omega_P^{\perp}$, obtained using the FPLAPW method, are given in Table II. It is clear that a strong anisotropy is present.

The real parts $\epsilon_1^{\perp}(\omega)$ and $\epsilon_1^{\parallel}(\omega)$ are obtained using the Kramers-Kronig relations.[38] The reflectivity $R(\omega)$, absorption coefficient $I(\omega)$, refractive index $n(\omega)$, and extinction coefficient $k(\omega)$ in the crystal are related to the reflectivity at normal incidence by[38]

$$R^{\perp}(\omega)=\frac{n^{\perp}+ik^{\perp}-1}{n^{\perp}+ik^{\perp}+1},$$

$$I^{\perp}(\omega)=\sqrt{2}\omega[\sqrt{\varepsilon_1^{\perp}(\omega)^2+\varepsilon_2^{\perp}(\omega)^2}-\varepsilon_1^{\perp}(\omega)]^{1/2},$$

$$k^{\perp}(\omega)=I^{\perp}(\omega)/2\omega,$$

$$n^{\perp}(\omega)=(1/\sqrt{2})[\sqrt{\varepsilon_1^{\perp}(\omega)^2+\varepsilon_2^{\perp}(\omega)^2}+\varepsilon_1^{\perp}(\omega)]^{1/2},$$

with similar expressions for the parallel component.

Figures 2(a)–2(c) show the calculated $\epsilon_2^{\perp}(\omega)$ and $\epsilon_2^{\parallel}(\omega)$ for $1T$-TiX_2 (X=S,Se,Te) along with the experimental data of Bayliss and Liang.[29] We find that $\epsilon_2^{\perp}(\omega)$ and $\epsilon_2^{\parallel}(\omega)$ are anisotropic. The effect of the Drude term is significant for

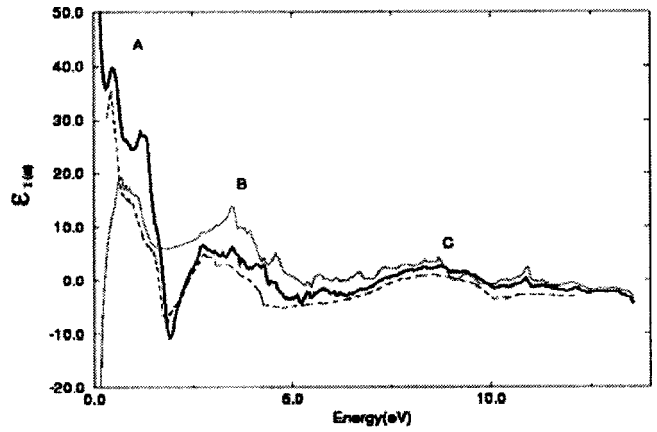

(a)

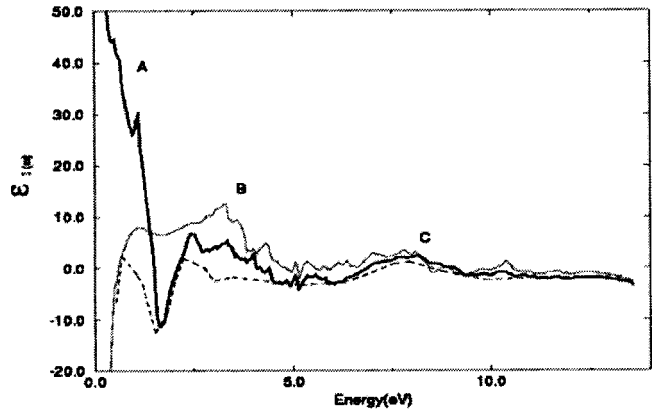

(b)

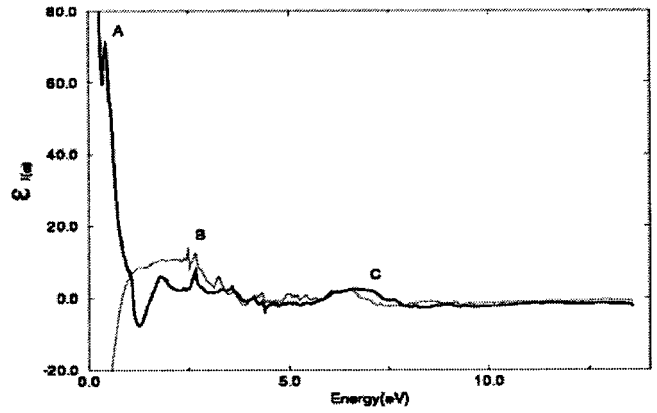

(c)

FIG. 3. Calculated $\epsilon_1^{\parallel}(\omega)$ (light line) and $\epsilon_1^{\perp}(\omega)$ (dark line) along with the experimental data (Ref. 29) (dashed line) for $\vec{E}\perp\mathbf{c}$. (a) $1T$-TiS, (b) $1T$-$TiSe_2$, and (c) $1T$-$TiTe_2$.

energies less than 1 eV. All the compounds show three main structures labeled A, B, and C. The location of these structures in the $1T$-TiX_2 compounds is given in Table II. Structure A is dominated by transitions from a band just below E_F to band just above it in the Σ M direction. Structures B and C are dominated by transitions from top (and bottom) of the chalcogen p states to Ti d states. The calculation of Leventi-

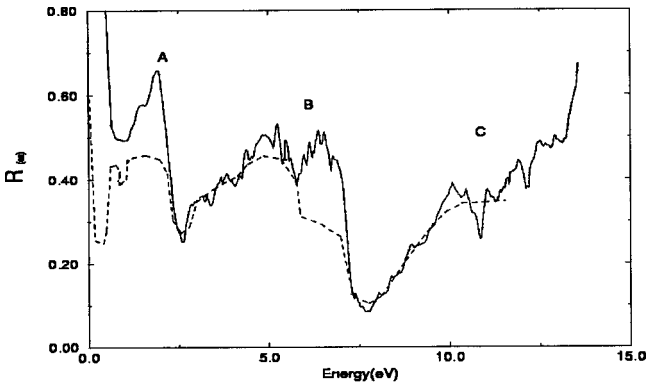

(a)

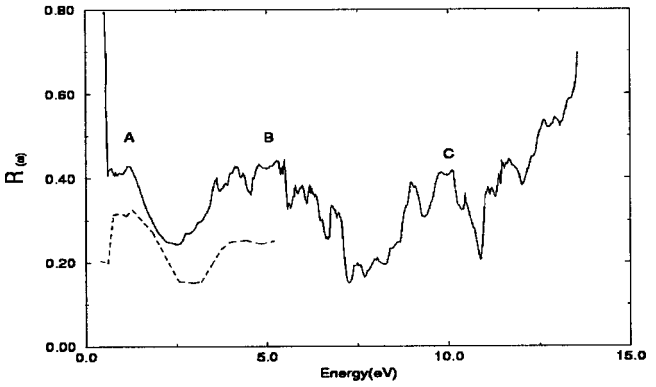

(b)

FIG. 4. Calculated reflectivity spectrum of $1T$-TiS_2 along with the experimental data (dashed line). (a) Greenway and Nitsche (Ref. 4) for $\vec{E}\perp\mathbf{c}$. (b) Bayliss and Liang (Ref. 28) for $\vec{E}\parallel\mathbf{c}$.

Peetz, Krasovskii, and Schattke[14] gives a larger peak height for structure A and the structure B is not so pronounced in $\epsilon_2^{\perp}(\omega)$ while the structure C is almost missing in $\epsilon_2^{\parallel}(\omega)$. We note that all the structures in optical response are shifted towards lower energies as we move from S to Se and Te, in agreement with the band structures.

$\epsilon_1^{\perp}(\omega)$ and $\epsilon_1^{\parallel}(\omega)$ for $1T$-TiX_2 are shown in Figs. 3(a)–3(c). In the low energy range the effect of Drude term is considerable. The calculated $\epsilon_1(\omega)$ is anisotropic. Once again main structures are discernible. The experimental data of Bayliss and Liang[29] for TiS_2 and $TiSe_2$ for $\vec{E}\perp\mathbf{c}$ shows good agreement with our calculations.

In order to make more detailed comparison with the experimental data, we have calculated the frequency dependent reflectivity and absorption coefficient. The reflectivity spectra for $\vec{E}\perp\mathbf{c}$ and $\vec{E}\parallel\mathbf{c}$ for TiS_2 and $TiSe_2$ along with the experimental data[4,28] are shown in Figs. 4 and 5. A considerable anisotropic is found. Figure 6 shows that the calculated reflectivity of $TiTe_2$ for $\vec{E}\perp\mathbf{c}$ is in agreement with the experimental data.[4] We have calculated the frequency-dependent absorption coefficient $I(\omega)$ and compare it with the experimental data[7] in Fig. 7. These also show three structures as in the case of $\epsilon_2^{\perp}(\omega)$ and $\epsilon_2^{\parallel}(\omega)$.

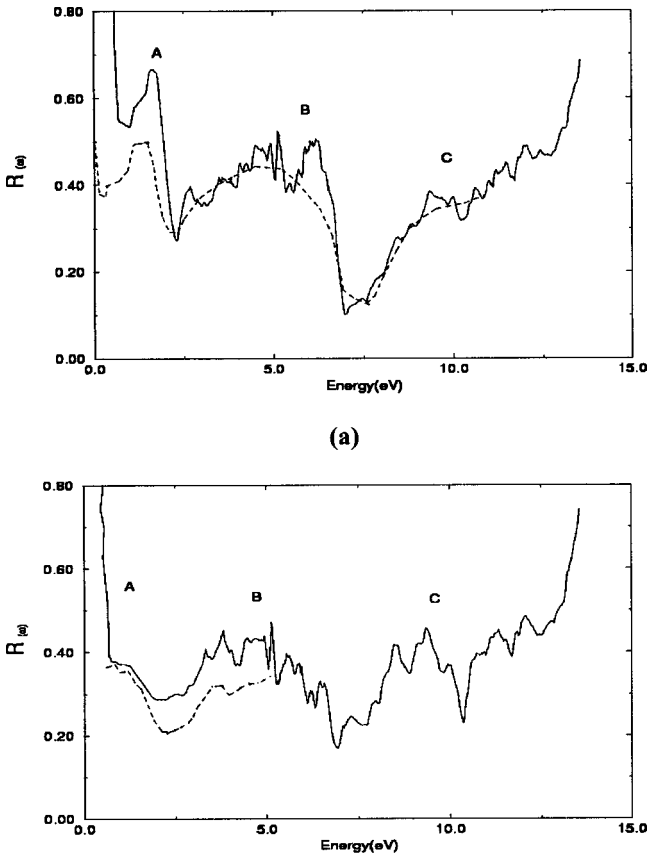

FIG. 5. Reflectivity spectrum of $1T$-$TiSe_2$ along with the experimental data (dashed line). (a) Greenway and Nitsche (Ref. 4) for $\vec{E}\perp\mathbf{c}$. (b) Bayliss and Liang (Ref. 28) for $\vec{E}\|\mathbf{c}$.

V. CONCLUSIONS

We have calculated the electronic and optical properties of $1T$-TiX_2 (X=S,Se,Te) and find these are semimetallic because of the overlap between the Ti $3d$ and the chalcogen p bands.[20] The Fermi energy usually lies in the chalcogen p cluster. The DOS at E_F increases in going from S to Te. This can be explained by increase in the overlap between the chalcogen p and Ti $3d$ bands. The variation of $N(E_F)$ with different methods suggests the inaccuracies inherent in non-full-potential methods. Although we have not compared our DOS with the x-ray photoelectron spectra, such a comparison has been made by many authors[14,23,40] and they obtain agreement. Since our DOS agrees with the DOS calculated by these workers[14,23,40] we expect our DOS to agree with the x-ray photoelectron spectra also.

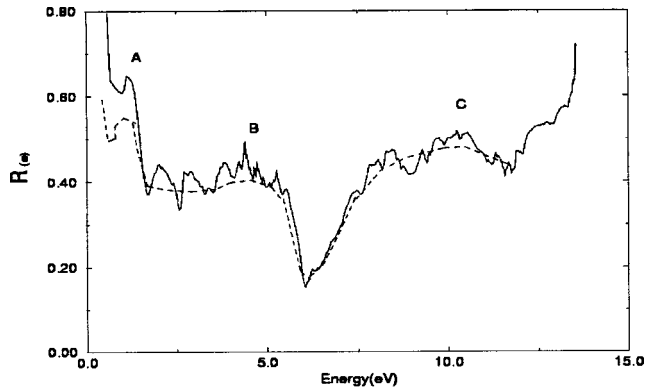

FIG. 6. Calculated reflectivity spectrum of $1T$-$TiTe_2$ along with the experimental data (dashed line) for Greenway and Nitcshe (Ref. 4) for $\vec{E}\perp\mathbf{c}$.

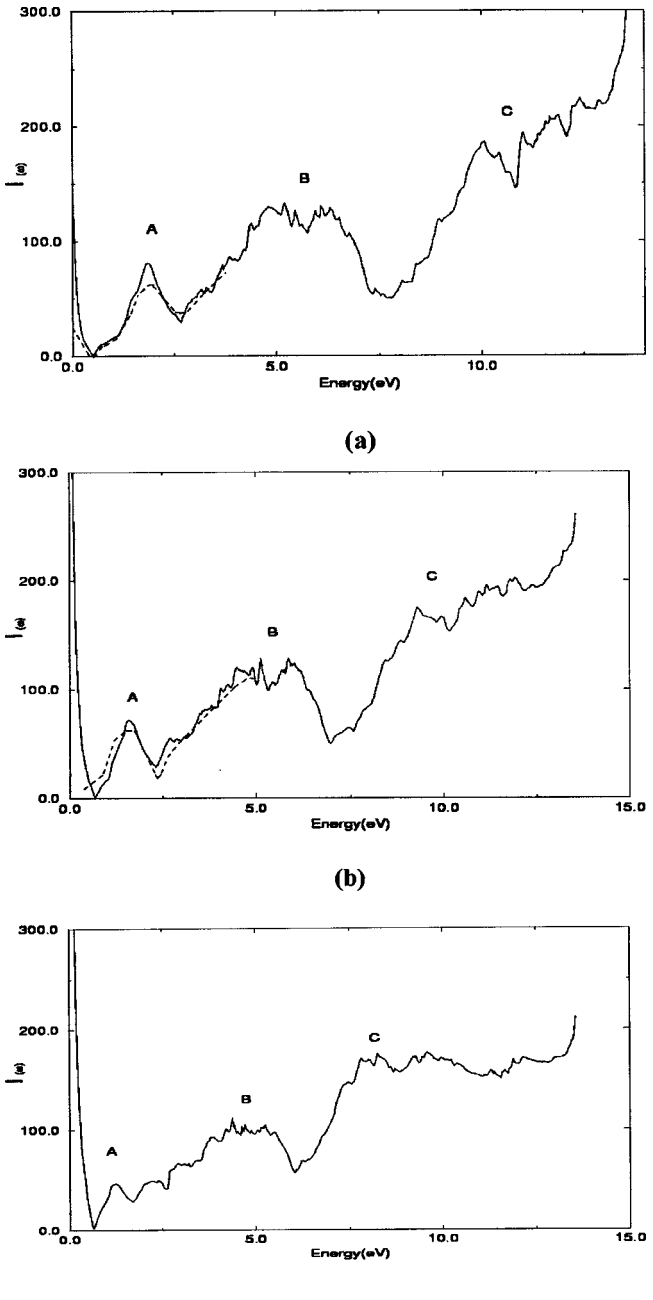

FIG. 7. Calculated absorption coefficient along with the experimental data (dashed line) for Murray and Yoffee (Ref. 7) for $\vec{E}\perp\mathbf{c}$. (a) $1T$-TiS_2, (b) $1T$-$TiSe_2$, and (c) $1T$-$TiTe_2$.

We have calculated the frequency dependent dielectric functions and find considerable anisotropy. The effect of the Drude term is important at energies less than 1 eV. In the energy range (<5 eV) the perpendicular component domi-

nates while in the high-energy range (>5 eV) both polarizations contribute. The frequency-dependent dielectric functions show three main structures arising primarily from band transitions from the chalcogen p valence states to the Ti $3d$ conduction states. We compare our calculated frequency dependent dielectric functions with the experimental data of Bayliss and Liang[29] and find good agreement. We have also calculated the frequency dependent reflectivity and the absorption coefficient. The behavior of these quantities is similar to the dielectric function in terms of anisotropy and structure. The agreement of our calculated and measured frequency dependent optical properties reiterates our belief in the accuracy of using full potential methods for optical properties and the necessity of using them. The only other calculation based on the ELAPW method does not show such encouraging results because they use muffin-tin approximation. Table II summaries the effect of X on the location of the peaks in optical spectra A, B, and C in TiX_2 compounds. We hope that our work would lead to more measurements of anisotropy of the optical properties.

ACKNOWLEDGMENT

We would like to thank the Institute Computer Center and Physics Department for providing the computational facilities.

[1] J. A. Wilson and A. D. Yoffe, Adv. Phys. **18**, 193 (1969).
[2] M. S. Whittingham, Science **192**, 1126 (1976).
[3] G. Umrigar, D. E. Ellis, D. S. Wang, H. Krakauer, and M. Posternak, Phys. Rev. B **26**, 4935 (1982).
[4] D. L. Greenway and R. T. Nitsche, Phys. Chem. Solids **26**, 1445 (1965).
[5] A. R. Beal, J. C. Knights, and W. Y. Liang, J. Phys. C **5**, 3531 (1972).
[6] W. Y. Liang, G. Lucovsky, R. M. White, and W. Stutius, Philos. Mag. **33**, 493 (1976).
[7] R. B. Murray and A. D. Yoffe, J. Phys. C **5**, 3038 (1972).
[8] P. C. Klipstein and R. H. Friend, J. Phys. C **17**, 2713 (1984).
[9] G. A. Benesh, A. M. Woolley, and C. Umrigar, J. Phys. C **13**, 1595 (1985).
[10] C. M. Fang, R. A. de Groot, and C. Haas, Phys. Rev. B **56**, 4455 (1997).
[11] Z. Y. Wu, G. Ouvrard, S. Lemaux, P. Moreau, P. Gressier, F. Lemoigno, and J. Rouxel, Phys. Rev. Lett. **77**, 2101 (1996); Z. Y. Wu, F. Lemoigno, P. Gressier, G. Ouvrard, P. Moreau, J. Rouxel, and C. R. Natoli, Phys. Rev. B **54**, R11 009 (1996).
[12] Z. Y. Wu, G. Ouvrard, P. Moreau, and C. R. Natoli, Phys. Rev. B **55**, 9508 (1997).
[13] D. R. Allan, A. A. Kelsey, S. J. Clark, R. J. Angel, and G. J. Ackland, Phys. Rev. B **57**, 5106 (1998).
[14] E. E. Leventi-Peetz, Krasovskii, and W. Schattke, Phys. Rev. B **51**, 17 965 (1995).
[15] Y.-S. Kim, M. Mizuno, I. Tanaka, and H. Adachi, Jpn. J. Appl. Phys. **37**, 4878 (1998).
[16] S. Sharma, T. Nautiyal, G. S. Singh, S. Auluck, P. Blaha, and C. Ambrosch-Draxl, Phys. Rev. B **59**, 14 833 (1999).
[17] S. Bocharov, G. Drager, D. Heumann, A. Simunek, and O. Sipr, Phys. Rev. B **58**, 7668 (1998).
[18] A. Simunek, O. Sipr, S. Bocharov, D. Heumann, and G. Drager, Phys. Rev. B **56**, 12 232 (1997).
[19] D. W. Fischer, Phys. Rev. B **8**, 3576 (1973).
[20] A. Borghesi, Tia Chen Chen, G. Guizzetti, L. Nosenza, E. Reguzzoni, A. Stella, and F. Levy, Phys. Rev. B **33**, 2422 (1984).
[21] N. Nagaosa and E. Hanamura, Phys. Rev. B **29**, 2060 (1984).
[22] R. Claessen, R. O. Anderson, G. H. Gweon, and J. W. Allen, Phys. Rev. B **54**, 2453 (1996).
[23] D. K. G. de Boer, C. F. van Bruggen, G. W. Bus, R. Coehoorn, C. Hass, G. A. Sawatzky, H. W. Myron, D. Norman, and H. Padmore, Phys. Rev. B **29**, 6797 (1984).
[24] K. Rossnagel, L. Kipp, M. Skibowski, C. Solterbeck, T. Strasser, W. Schattke, D. VoB, P. Kruger, A. Mazur, and J. Pollmann, Phys. Rev. B **63**, 125104 (2001).
[25] L. Perfetti, C. Rojas, A. Reginelli, L. Gavioli, H. Berger, G. Margaritondo, and M. Grioni, Phys. Rev. B **64**, 115102 (2001).
[26] T. E. Kidd, T. Miller, M. Y. Chou, and T.-C. Chiang, Phys. Rev. Lett. **88**, 226402 (2002).
[27] H. P. Hughes and W. Y. Liang, J. Phys. C **10**, 1079 (1977).
[28] S. C. Bayliss and T. Liang, J. Phys. C **15**, 1283 (1982).
[29] S. C. Bayliss and W. Y. Liang, J. Phys. C **18**, 3327 (1985).
[30] A. Borghesi, B. Guizzetti, L. Nosenzo, E. Reguzzoni, and A. Stalla, Nuovo Cimento D **4**, 141 (1984).
[31] L. Baldassare, A. Cingdani, and F. Levy, Opt. Commun. **71**, 72 (1989).
[32] P. Blaha, K. Schwarz, and J. Luitz, WIEN97, Vienna University of Technology (1997) [improved and updated unix version of the original copywright WIEN code] which was published by P. Blaha, K. Schwartz, P. Sorantin, and S. B. Trickey, Comput. Phys. Commun. **59**, 399 (1990)].
[33] U. Von Barth and L. Hedin, J. Phys. C **5**, 1629 (1972).
[34] S. Sharma, Claudia Ambrosch-Draxl, M. A. Khan, P. Blaha, and S. Auluck, Phys. Rev. B **60**, 8610 (1999).
[35] O. Jepsen and O. K. Andersen, Solid State Commun. **9**, 1763 (1971); G. Lehmann and M. Taut, Phys. Status Solidi B **54**, 496 (1972).
[36] T. Yamasaki, N. Suzuki, and K. Motizuki, J. Phys. C **20**, 395 (1987).
[37] Sangeeta Sharma, S. Auluck, and M. A. Khan, Pramana J. Phys. **54**, 431 (2000).
[38] F. Wooten, *Optical Properties of Solids* (Academic, New York, 1972).
[39] B. Chakraborty, W. E. Pickett, and P. B. Allen, Phys. Rev. B **14**, 3227 (1972).
[40] A. Fujimori, S. Suga, H. Negishi, and M. Inoue, Phys. Rev. B **38**, 3676 (1988).
[41] W. J. L. Buyers and B. M. Powell, Can. J. Phys. **58**, 207 (1980).